A Study of Active Shifting of Human Driver for Improving Wheelchair Tipping Stability

William W. Li, Shahram Payandeh
Experimental Robotics Laboratory (ERL), School of Engineering Science
Simon Fraser University, Burnaby, British Columbia, Canada V5A 1S6
Fax: (604) 291-4951

Abstract

This paper presents a model describing the effects of a human driver on the tipping stability of a powered wheelchair. The tipping stability is measured by the angle of tilt required to induce a loss of contact between any of the wheels of the wheelchair and the ground. Specifically, the effect of moving the centre of gravity of the human driver relative to that of the wheelchair in a controlled manner is shown to improve the tipping stability. Expressions are derived relating the static and dynamic tipping criteria to the position and relative mass of the human. A simple controller is used to demonstrate that this strategy serves to improve tipping stability.

1. Introduction

Independence is one of the key factors which contribute to quality of life. According to [1], mobility along with communication play a critical role in maintaining independence, and the degree of mobility is directly related to one's level of independence. Powered wheelchairs are the primary means by which many physically disabled people extend the limits of their mobility both in and out of their home and work environments. These limits, though, are circumscribed by the range of places the wheelchairs can safely take the user. Common physical limits to mobility include sidewalk curbs, stairs, and sloped roads. In many such situations, the limitation is not imposed by the ability of the wheelchair itself to negotiate the terrain so much as by the safety and comfort of the driver as the wheelchair changes attitude in traversing the terrain.

Powered wheelchairs can be thought of as small vehicles in which the driver sits (Figure 1). Like an automobile, the powered wheelchair possesses (usually) four wheels, motors, and a battery pack. The driver steers the wheelchair through a control interface mounted either on the armrest or headrest. Unlike the common car, though, the driver makes up a significant fraction of the total loaded vehicle weight. An adult might weigh 65 kg or more. Together with the seat (~18 kg) which the driver is usually belted into, about half of the total weight of a typical loaded powered wheelchair (occupant plus wheelchair) is composed of or directly attached to the driver. For ergonomic reasons, the driver must be kept a reasonable height off the ground, raising the person's centre of gravity (CoG) and subsequently the CoG of the loaded wheelchair. At the same time, the footprint of the wheelchair must be kept small enough to allow for easy maneuverability (e.g., egress through doorways). The result is a compromise between size and maneuverability and structural stability.

This paper deals primarily with powered wheelchairs, although some of the results may be more generally applicable.

Data gathered by [2] suggests that tipping is one of the biggest concerns for wheelchair users in motion. As defined in the ISO standards on wheelchair stability [3][4], tipping stability is associated with the loss of driver control over the wheelchair's behaviour inherent in the lifting of one or more wheels, as it is through the wheels of the vehicle that the wheelchair is steered and driven.

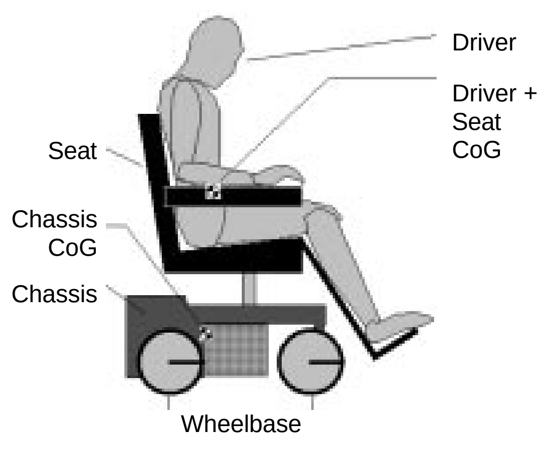

Figure 1: Powered wheelchair nomenclature.

Knowing when one or more wheels lose contact with the ground is important because the wheels are necessary for control of the direction of the wheelchair's direction, especially in turning on a slope, as pointed out in [5]. Furthermore, the loss of even one contact point out of the four which most powered wheelchairs have can cut down the tipping stability drastically by reducing the effective footprint covered by the wheelchair, as [6] has noted.

In the static stability test [3], a fully-loaded wheelchair (including a test dummy as the driver) is placed upon a tiltable platform. The wheelchair is gently tilted in several different directions and the stability limit recorded for each. The stability limit for a particular configuration (e.g., locked brakes, wheelchair facing downhill) is defined as the tilt angle at which one or more wheels of the wheelchair slide along the platform due to insufficient friction between the wheel and the test plane or where the wheelchair tips over.

The dynamic stability test [4] is similar, with the exception being that the wheelchair is accelerated and braked going up and down, respectively, a tilted surface. The stability limit is again defined by the tilt angle at which the wheels are observed to lift off the surface in braking or accelerating or where the wheelchair tips over.

Another related issue is the loss of upright posture, which can have negative consequences for the driver ranging from discomfort to loss of control over the wheelchair. People who use powered wheelchairs do so because they do not have the requisite upper body strength or endurance to use a manual wheelchair, and hence may not to be able to bring their bodies back to an upright position if their own position in their seats changes as a result of an attitudinal change in the wheelchair chassis. [7] Additionally, although most wheelchair drivers will have seatbelts and hence are in little danger of sliding out of their seats, a tilted seat will result in uncomfortable and potentially physiologically harmful shear forces at the bearing skin surfaces. In fact, devices such as [8] have been designed specifically to combat such debilitating effects.

Logically, the ability to shift the driver relative to the wheelchair chassis should aid in maintaining structural stability, by changing the vehicle geometry to compensate for the terrain. Indeed, wheelchairs such as [9] which allow for such a function are already in existence. Automatic compensation, however, has primarily been the domain of larger vehicles such as [10]. Other authors [12]-[15] have suggested that such a shift can have large effects on the stability of the wheelchair, in the case of manual wheelchairs. The next sections present a simple model for loaded wheelchairs and present some criteria for evaluating tipping stability based on measured geometry. Lastly, a mechanism for effecting the movement of the driver and seat is presented.

2. Modeling

In this paper, some of the conditions which lead to tipping, as well as some simplified models which can be used to predict tipping, will be developed. The primary model which will be used is a two-dimensional one where a 65 kg human is sitting on a Fortress Scientific electric wheelchair, as pictured in Figure 1. The masses of the various portions of the wheelchair were derived from experimental measurements. The mass distribution model of the human was supplied with the two-dimensional mechanical simulation software [16], which is shown to be substantially the same as [17].

Because the criteria used to evaluate tipping stability [3][4] deal with motion and structural stability in a single direction at a time, the models presented in this paper are fairly simple two-dimensional ones. Given decoupling of pitch (forward/back rotation) and roll (rotation left/right), these two-dimensional models may be applied to certain three-dimensional cases, such as the ISO tip stability testing procedures [3][4].

2.1 Single-Mass Model

The loaded wheelchair can be modeled as a single mass M, with a moment of inertia I_{cm} about its centre of mass. The forces acting on M are the gravitational force $M\vec{g}$, the surface normal reaction forces $\vec{N}_1$ and $\vec{N}_2$, and the frictional forces $\vec{F}_{f1}$ and $\vec{F}_{f2}$ with coefficients of friction μ_1 and μ_2.

The displacement vector $\vec{r}_{cm}$ to the centre of mass is given by the column vector:

$$\vec{r}_{cm} = \begin{bmatrix} \cos\theta & \sin\theta \\ -\sin\theta & \cos\theta \end{bmatrix} \begin{bmatrix} -l_1 \\ h \end{bmatrix} \qquad (1.a)$$

while the vector $\vec{r}_{12}$ from the downhill contact point to the uphill contact is similarly given by:

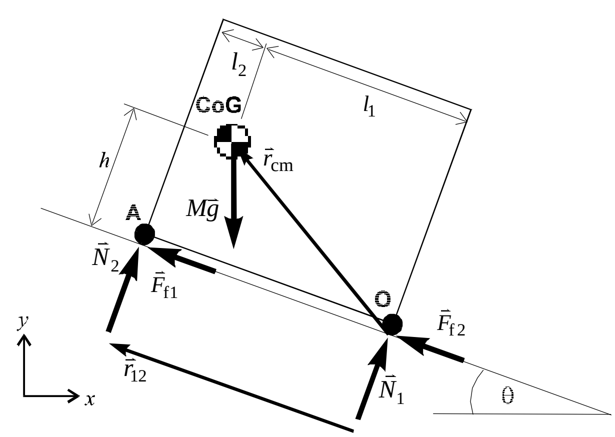

Figure 2: Single-Mass Wheelchair Model

$$\vec{r}_{12} = \begin{bmatrix} \cos\theta & \sin\theta \\ -\sin\theta & \cos\theta \end{bmatrix} \begin{bmatrix} -(l_1 + l_2) \\ 0 \end{bmatrix} \qquad (1.b)$$

The model shown in Figure 2 serves equally well for analysis of transverse (side-slope) and longitudinal (down-slope) problems. In this model, there are only two points of contact with the slope at **O** and **A**, each corresponding to one pair of wheels. (e.g., in a longitudinal problem, the points of contact are the front and back pairs of wheels.)

We can disregard any moment of inertia of the wheels, as the wheels tend to be quite small on powered wheelchairs and turn relatively slowly, and hence possess a negligible moment as compared with the rest of the system.

2.2 Two-Mass Model

An extension of the single-mass model separates the driver and seat from the chassis (Figure 3). In many powered wheelchairs, the seat is customized or capable of being customized to suit the needs of the user, separate from the chassis which contains the motors, wheels, and batteries. It is a practical approach to insert a mechanism between the seat and the chassis in order to position the seat and driver for maximal tipping stability.

In the two-mass model, the mass of any linkages which connect the driver to the chassis mass has been disregarded as negligible compared to the mass of the rest of the system.

For a given configuration of the two masses, we can calculate a single-mass equivalent using:

$$\vec{r}_{\mathrm{cm}} = \frac{m_{\mathrm{c}}}{M}\vec{r}_{\mathrm{c}} + \frac{m_{\mathrm{d}}}{M}\left(\vec{r}_{\mathrm{c}} + \vec{r}_{\mathrm{c}\to\mathrm{d}}\right) = \vec{r}_{\mathrm{c}} + \frac{m_{\mathrm{d}}}{M}\vec{r}_{\mathrm{c}\to\mathrm{d}} \qquad (2.a)$$

$$M = m_{\mathrm{c}} + m_{\mathrm{d}} \qquad (2.b)$$

which gives us the centre of mass for the combined system.

The distribution of mass in the seated human locates the CoG of the combined driver and seat system as located in Figure 1, at the ventral surface of the lower abdomen. (Exact position depends on the individual driver.)

2.3 Equivalence of Tilt and Acceleration in Tipping Stability

Consider the case of a wheelchair accelerating to the left on a level plane, as shown in Figure 4. A reference frame attached to the wheelchair would be non-inertial due to the acceleration. An inertial frame can be constructed by the addition of a fictitious external force of magnitude $M\ddot{x}$ acting in the opposite direction of the acceleration. The resulting configuration, pictured on the right side of Figure 4, is analogous to the static tilted models with a slightly larger force $\vec{F}$ replacing the gravitational force $M\vec{g}$ from the model of Figure 2. The incline angle $\theta_{\mathrm{o}} = \theta_{\mathrm{a}}$, the included angle between the vectors $M\vec{g}$ and $M\ddot{x}$. It is not difficult to see by inspection that acceleration on a slope θ can be modeled with a mass on an incline with an angle equal to the sum of θ_{a} and θ. Thus, the analysis of the wheelchair on an incline presented here can be applied to more general situations.

As an example, we can obtain the side tipping, or roll, stability, by considering the addition of centripetal acceleration to the wheelchair. To model this acceleration using the static model, we can add a centrifugal pseudo-force in the x-direction to the gravitational force pulling down on the system, in similar fashion to [6], and considering this system to be quasi-static. This new setup can then be used to calculate roll stability. In a three-dimensional model which would extrapolate from this work, it is essential that consideration be taken of roll as well as pitch stability.

3. Static Tipping Stability

Although the tipping stability of the wheelchair is measured by the angle of tilt required to actually tip the

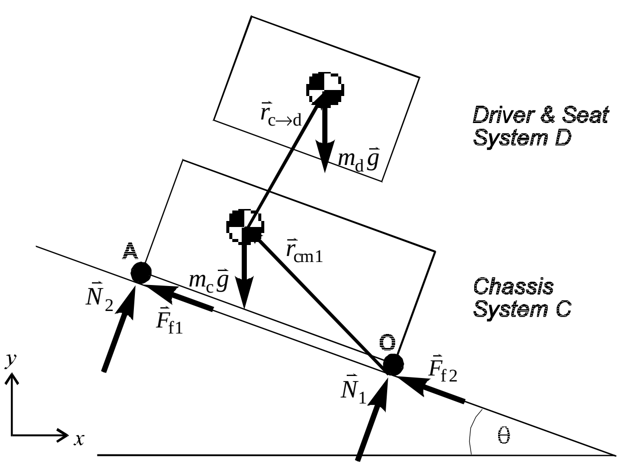

Figure 3: Two-Mass Wheelchair Model

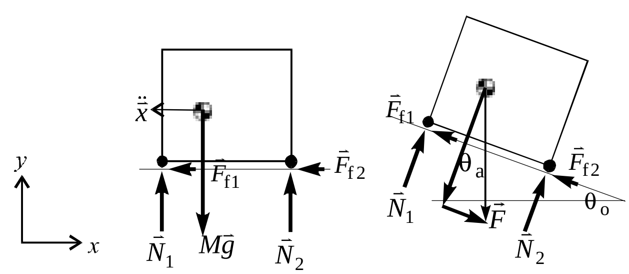

Figure 4: Accelerating vs. Tilted Frames

wheelchair, it can also be applied to more general situations as a margin to unrecoverable tipping. Recoverable tipping of the wheelchair ends up with the wheelchair returning to its original position and orientation, while unrecoverable tipping leads to rather catastrophic results.

3.1 Static Tipping Criterion

As a first step in calculating the tipping stability limits of the model, in a derivation similar to [12], consider the sums of forces and moments in the model shown in Figure 2. In the static situation, these sums will be identical to $\vec{0}$. Assuming that $l_1 < l = l_1 + l_2$ (l, the distance between the two contact points, is fixed for a given system configuration.) and that $\theta \geq 0$, the point of rotation will be about the downhill contact point **O**. $\vec{N}_1$, $\vec{F}_{f1}$, and $\vec{F}_{f2}$ act through **O**, and hence do not contribute a moment in equation (4).

$$\vec{0} = \vec{N}_1 + \vec{N}_2 - M\vec{g} \quad (3)$$

$$\vec{0} = (\vec{r}_{cm} \times M\vec{g}) + (\vec{r}_{12} \times \vec{N}_2) \quad (4)$$

Equation (3) can be rewritten in terms of its components. Specifically, we look at the component of force along the direction normal to the ramp surface:

$$0 = \left|\vec{N}_1\right| + \left|\vec{N}_2\right| - \left|M\vec{g}\right|\cos\theta \quad (5)$$

Equation (4) will have a z-component only, perpendicular to the two-dimensional model plane:

$$0 = Mg(-l_1\cos\theta + h\sin\theta) - (l_1 + l_2)\left|\vec{N}_2\right| \quad (6)$$

At the limit of stability, $\vec{N}_2 = \vec{0}$ as point **A** just lifts away from the ground, so equation (6) simplifies into:

$$\tan\theta_{crit} = {}^{l_1}\!/_{h} \quad (7)$$

Equation (7) gives the tipping stability limit, the angle θ_{crit} at which the wheelchair first starts to tip over. As pointed out in [6], this static tipping stability criterion can also be applied to roll stability while turning, by adding an extra centrifugal force component applied at the CoG, which will contribute additional tipping moment.

3.2 Relationship Between System Centre of Gravity and Tipping Stability

For a given configuration of the single-mass model, the location of the system CoG is fixed. With the two-mass model, though, we are able to move the system CoG by moving system D relative to system C. Because the mass of the driver-seat system is roughly equivalent to that of the chassis, equation (2.a) suggests that for any given movement of system D relative to system C, the system CoG will move half as much in the same direction. We will make use of this property in order to actively shift the system CoG to maximize tipping stability by maximizing the zone of stability.

It is apparent from equation (7) that an increased height h of the CoG above the ground will lower θ_{crit} and hence decrease the tipping stability, which is an intuitively obvious result. Furthermore, increasing the horizontal displacement l_1 of the CoG seems to increase the θ_{crit}. However, one cannot increase l_1 without bound.

For $l_1 < l$, the wheelchair retains tipping stability for the one-sided zone of stability $\theta \in [0, \theta_{crit}]$. If one makes $l_1 > l$, though (forcing relative displacement l_2 negative), the region of stability flips around to $[\theta_{crit}, \pi/2]$, which is not generally desirable. This fits with simple physics and the observations of [6] that the CoG must remain within the footprint formed by the projection of the bounded area between the ground contact points onto the horizontal plane.

Because $l = l_1 + l_2$, increasing the system l_1 by moving mass D decreases the system l_2. It is possible to calculate a tipping stability criterion for the uphill side, which will give us a two-sided zone of stability $\theta \in [-\theta_{crit2}, \theta_{crit1}]$ where

$$\tan(\theta_{crit2}) = \frac{l - l_1}{h} = \tfrac{\pi}{2} - \theta_{crit1} \quad (8)$$

as long as $l_1 < l$. The total zone of stability will be given by:

$$\theta_{crit1} + \theta_{crit2} = \tfrac{\pi}{2} \quad (9)$$

For a given chassis tilt angle θ_c, the optimal stability zone is chosen such that θ_c is equidistant from the two stability limit angles. This choice will be given by choosing the parameters such that:

$$\theta_c = \tfrac{1}{2}(\theta_{crit1} - \theta_{crit2}) = \theta_{crit1} - \tfrac{\pi}{4} \quad (10)$$

which will center the system CoG inside the wheelchair's footprint.

4. Formulation of Dynamic Tipping Stability

In the dynamic stability test of [4], the wheelchair is braked suddenly going downhill. In the worst case, the wheelchair comes to a sudden halt rather than decelerating smoothly, similar to impact with a low

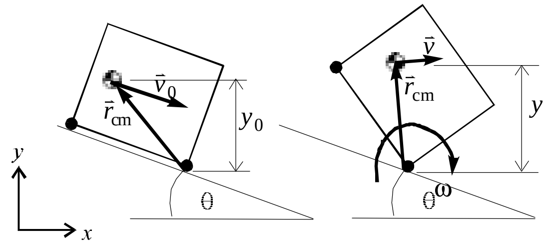

Figure 5: Wheelchair plastic collision

obstacle going downhill, as in Figure 5. In such a case, the rear wheels of the wheelchair will definitely leave the ramp. We will determine the response to this impulse input by looking at the extent to which the wheelchair tips and the conditions required for such tipping.

In this section, the following definitions apply:

- T total kinetic energy
- V potential energy
- v translational speed
- ω rotational speed
- y height of CoG in world coordinates

Subscript 0 refers to the situation immediately prior to impact, subscript 1 refers to the situation immediately after impact, and subscript 2 refers to the situation some time after impact.

4.1 Threshold Unrecoverable Tipping Speed

Consider a wheelchair moving downhill with a translational speed v_0 and rotational speed ω_0=0 when the brakes are applied. In such a case, we can find the speeds v_1 and ω_1 immediately post-impact by summing the system momenta before and after the impact [18]. As this is a plastic collision, we apply the principle of conservation of angular momentum:

$$(Mv_0)h = (Mv_1)|\vec{r}_{\mathrm{cm}}| + I_{\mathrm{cm}}\omega_1 \tag{11}$$

Because the wheelchair starts rotating about the point of impact, we consider that $v_1 = |\vec{r}_{\mathrm{cm}}|\omega_1$. Combining this expression with equation (11) leads to:

$$Mv_0 h = \left(I_{\mathrm{cm}} + M|\vec{r}_{\mathrm{cm}}|^2\right)\omega \tag{12}$$

which gives us an expression for the total kinetic energy post-impact:

$$\begin{aligned} T_1 &= \tfrac{1}{2} M v_1^2 + \tfrac{1}{2} I_{\mathrm{cm}}\omega_1^2 \\ &= \tfrac{1}{2}\left(I_{\mathrm{cm}} + M|\vec{r}_{\mathrm{cm}}|^2\right)\omega_1^2 \end{aligned} \tag{13}$$

Note that the wheelchair has lost some of its kinetic energy to the plastic collision, so that in general $T_1 < T_0$. We will comment more on this fact in the next section.

We can calculate the conditions required to induce unrecoverable tipping of the wheelchair, where the wheelchair's tilt angle in world coordinates has reached the limit of static stability θ_{crit} with zero speed. Tipping of the wheelchair up to this point will be recoverable, as the wheelchair will be statically stable even at maximum tip, and hence recover its initial position and orientation. If the initial kinetic energy is enough to push the wheelchair past this point, then the wheelchair will have no static stability.

It is desirable to maximize this threshold, so that for any given braking situation, one will have the maximum possible margin to unrecoverable tipping.

Applying conservation of energy post-impact,

$$T_1 + V_1 = T_2 + V_2 \tag{14}$$

where V_1=Mgy_1 and V_1=Mgy_2. y_1=y_0 because the wheelchair hasn't moved yet immediately after the impact. In unrecoverable tipping, the wheelchair must pass through the position where $y_2 = |\vec{r}_{\mathrm{cm}}|$. Since we are trying to find the minimum speed which will lead to unrecoverable tipping, we will consider the case where T_2=0, i.e., where the wheelchair has just enough kinetic energy left after impact to raise the system to the threshold of unrecoverable tipping. Solving equation (14) for T_1 and substituting the expressions from equations (12) and (13) yields:

$$T_1 = \frac{\tfrac{1}{2}(Mv_0 h)^2}{I_{\mathrm{cm}} + M r_{\mathrm{cm}}^2} = Mg(y_2 - y_0) \tag{15}$$

The geometry in Figure 5 suggests that:

$$\begin{aligned} y_0 &= |\vec{r}_{\mathrm{cm}}|\sin\left(\theta + \tfrac{\pi}{2} - \theta_{\mathrm{crit}}\right) \\ &= |\vec{r}_{\mathrm{cm}}|\cos\left(\theta_{\mathrm{crit}} - \theta\right) \end{aligned} \tag{16}$$

At the threshold of tipping, $y = r_{\mathrm{cm}}$. Substituting into equation (15) along with equation (16), and solving for $v_{\mathrm{thresh}} = v_0$ gives us:

$$v_{\mathrm{thresh}} = \sqrt{\frac{2g|\vec{r}_{\mathrm{cm}}|}{Mh^2}\left(I_{\mathrm{cm}} + M|\vec{r}_{\mathrm{cm}}|^2\right)\left(1 - \cos\left(\theta_{\mathrm{crit}} - \theta\right)\right)} \tag{17}$$

Equation (17) is an expression for the maximum speed the wheelchair can be travelling at when the brakes are applied past which the wheelchair will tip completely over in an unrecoverable fashion. As expected, increasing the slope angle θ or the height of the system CoG h will decrease v_{thresh}.

The system moment of inertia I_{cm} is related to the moments of inertia I_{c} and I_{d} of the two components of the two-mass model through the parallel-axis theorem and judicious application of equation (2):

$$\begin{aligned} I_{\mathrm{cm}} &= I_{\mathrm{c}} + I_{\mathrm{d}} + m_{\mathrm{c}}|\vec{r}_{\mathrm{cm}} - \vec{r}_{\mathrm{c}}|^2 + m_{\mathrm{d}}|\vec{r}_{\mathrm{cm}} - \vec{r}_{\mathrm{d}}|^2 \\ &= I_{\mathrm{c}} + I_{\mathrm{d}} + \frac{m_{\mathrm{c}} m_{\mathrm{d}}}{m_{\mathrm{c}} + m_{\mathrm{d}}}|\vec{r}_{\mathrm{c}\to\mathrm{d}}|^2 \end{aligned} \tag{18}$$

The implication of equation (18) is that by increasing the separation $|\vec{r}_{\mathrm{c}\to\mathrm{d}}|$ of the two component masses, we can increase I_{cm} and hence the resistance of the wheelchair to tipping. Furthermore, we get a double effect on v_{thresh}, as increasing $|\vec{r}_{\mathrm{c}\to\mathrm{d}}|$ will also increase $|\vec{r}_{\mathrm{cm}}|$ in equation (17).

4.2 Maximum Tip Criterion

Another criterion we can use is the maximum amount of tip Δy which is generated upon braking, which is a measure of how much time the wheelchair's wheels spend off the ground and out of play as control surfaces for the wheelchair. It is desirable to minimize Δy as decreasing the amount of time the wheelchair's wheels spends away from the grounds increases the control the driver has over a given braking situation. $\Delta y = y_2 - y_0$, so from equations (15) and (16):

$$\begin{aligned}\Delta y &= \frac{M v_0^2 h^2}{2g\left(I_{\mathrm{cm}} + M\left|\vec{r}_{\mathrm{cm}}\right|^2\right)} \\ &= \frac{T_0}{g}\frac{h^2}{\left(I_{\mathrm{cm}} + M\left|\vec{r}_{\mathrm{cm}}\right|^2\right)}\end{aligned} \qquad (19)$$

Note that equation (19) is independent of the ramp angle θ. It is only the amount of kinetic energy on impact which affects the height Δy which the wheelchair gains.

We can rewrite equation (19) in more usable terms if we recall from the single-mass model that $\left|\vec{r}_{\mathrm{cm}}\right|^2 = h^2 + l_1^2$. Applying this expression for $\left|\vec{r}_{\mathrm{cm}}\right|^2$ to equation (19) we get the ratio of change in potential energy ΔU at maximum tilt to kinetic energy on impact:

$$\begin{aligned}\frac{\Delta U}{T_0} &= \frac{M h^2}{\left(I_{\mathrm{cm}} + M\left|\vec{r}_{\mathrm{cm}}\right|^2\right)} \\ &= \frac{1}{1 + \left(\frac{I_{\mathrm{cm}} + M l_1^2}{M h^2}\right)} < 1\end{aligned} \qquad (20)$$

The ratio of equation (20) calculates the amount of the kinetic energy originally available which is not dissipated in the plastic collision, and hence the ratio is always less than unity. In the real world, the plastic collision in this model could correspond to braking via some dissipative friction process or to sudden stopping when hitting some irregularity in the ground such as a curb. It is obviously of benefit to have as much kinetic energy as possible dissipated in the braking process and as little as possible transformed into potential energy in raising the rear end of the wheelchair off the ground.

To decrease the ratio of equation (20), one notes that increases in the system moment of inertia I_{cm} and the horizontal displacement of the system CoG (relative to the baseline between the two ground contact points) l_1 both have a desirable (decreasing) effect on the ratio, while increasing the vertical displacement h has the expected undesirable effect (increasing the ratio). As I_{cm} will increase with increases in $\left|\vec{r}_{\mathrm{c}\to\mathrm{d}}\right|$, we can conclude that in order to increase the wheelchair tipping stability, we should increase $\left|\vec{r}_{\mathrm{c}\to\mathrm{d}}\right|$ in such a manner as to increase l_1 and decrease or keep constant h, so the primary adjustment is one of sliding the driver-seat system back-and-forth. It is still desirable, though, to have some rotation of the driver-seat system in order to reduce shear forces, as pointed out in section 1.

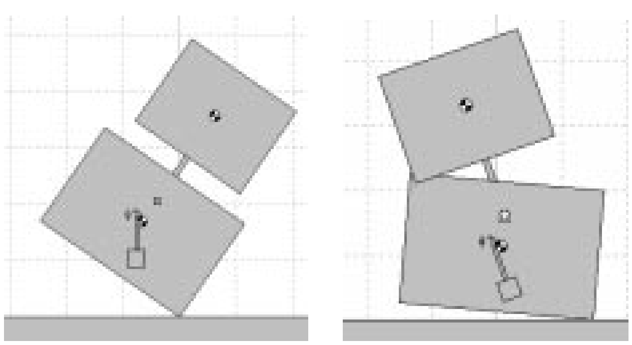

Figure 6: Simulation of Person on Wheelchair with Active Leveling

5. Effect of Active Control on Stability

According to [17], approximately half of the mass in humans (mean 56.5% percentage by weight among the population sampled) is located in the torso minus the limbs. As it is the torso which is secured into the seat, it is fairly safe to treat the driver and seat combination as one rigid body.

A simple simulation which can accomplish the goals of improving tipping stability and limiting shear forces on the driver is shown in the simulation trace of Figure 6. Here, the two-mass model has been used to demonstrate active control over system centre of gravity. Each simulation has been captured at the point of maximum system tilt. The model at the left has the two masses rigidly joined together, and is similar to the single-mass model. The model at the right has the second mass under active control.

The mass of system D in this model is 40 kg, with a moment of inertia of 27 kg m^{-2}, while the mass of system C is 48 kg, with a moment of inertia of 52 kg m^{-2}. The CoG of system D is 3.275 m off the ground, while the CoG of system C is 1.0 m off the ground. The l_1 parameter is 1.5 m. In both cases, the systems were started at a speed of 4.478 m/s, which is the threshold tipping speed for the rigid system.

The active mechanism itself consists of a powered rotational joint, similar to those found in manually-controlled tiltable wheelchair seats, which pitches the driver and seat back and forth. Because the driver-seat system CoG is 0.25m above this rotational joint, a rotation in either direction will have the effect of changing l_1 and decreasing h. Furthermore, the resulting change in attitude of the driver-seat system can be used to reduce shear forces if the alignment is such that the head of the driver is always pointed away from the net force vector on the system. The net force vector is a vector sum of gravitational pull combined with any forces experienced as a result of acceleration. The sensor used is a damped pendulum mounted on the wheelchair chassis. This pendulum allows the direct measurement of the net force vector on the wheelchair at any time.

Dynamically, the driver-seat system in this example behaves like an inverted pendulum, and a simple PD controller is used to control the tilt of the driver-seat system to match the tilt angle of the pendulum. As the comparison in Figure 6 shows, this simple controller does an adequate job of bringing the person to a gentle halt, although it is easy to imagine a better mechanism for absorbing the shock of stopping.

6. Summary and Conclusions

It is clear that the position of the human driver in a loaded powered wheelchair can have a large effect on the wheelchair's tipping stability. Expressions have been developed which allow one to determine how much margin a given wheelchair configuration has to tipping in static, quasi-static, and dynamic situations. Using these expressions, one can evaluate existing wheelchair configurations for their tipping stability as well as determine appropriate goals for control algorithms which actively shift the driver to maintain stability.

This work will contribute towards the development of a pitch-roll CoG stability-compensated suspension for use in wheelchairs, as the guideline for the envelope of motion of the suspension system. As the results of section 5 demonstrate, their are great potential benefits to utilizing such a suspension system. Work on a large motion active suspension system is currently in progress at SFU.

7. Acknowledgments

This work was funded by the Prototype Development Fund of the SFU University-Industry Liaison Office and through a grant from the Wighton Endowment Fund.

8. References

[1] C.G. Warren, "Powered mobility and its implications," J. Rehab. Res. Dev., Clinical Supplement #2, pp. 74-85, 1990.

[2] R.L. Kirby, S.A. Ackroyd-Stolarz, M.G. Brown, S.A. Kirkland, and D.A. MacLeod, "Wheelchair-related accidents caused by tips and falls among noninstitutionalized users of manually propelled wheelchairs in Nova Scotia," *Am. J. Phys. Med. Rehabil.*, vol. 73, no. 5, pp. 319-330, 1994.

[3] *Wheelchairs – Part 1: Determination of static stability.* Stockholm: International Organization for Standardization, 1986: ISO 7176-1.

[4] *Wheelchairs – Part 2: Determination of dynamic stability of electric wheelchairs.* Stockholm: International Organization for Standardization, 1990: ISO 7176-2.

[5] C.E. Brubaker, C.A. McLaurin, and I.S. McClay, "Effects of side slope on wheelchair performance," *J. Rehabil. Res. Dev.*, vol. 23, no. 2, pp. 55-57, 1986.

[6] R.A. Cooper and M. MacLeish, "Racing wheelchair roll stability while turning: a simple model," *J. Rehab. Res. and Dev.*, vol. 29, pp. 23-30, 1992.

[7] J. Vandyke, personal communication, May 2, 1994.

[8] J.M. Koerlin, J.L. Tausz, "Zero shear recliner/tilt wheelchair seat," U.S. Patent 5,297,021, Mar. 1994.

[9] G.G. Goertzen, N.J. Curran, and J.H. Molnar, "Powered wheelchair with adjustable center of gravity and independent suspension," U.S. Patent 5,575,348, Nov. 1996.

[10] G. Liprandi et al, "Anticentrifugal active lateral suspension for railway vehicles," U.S. Patent 5,454,329, Oct. 1995.

[11] S. Inagaki, S. Tagawa, "Active suspension with roll control by reducibly modified estimated transverse acceleration," U.S. Patent 5,384,705, Jan. 1995.

[12] G.G. Majaess, R.L. Kirby, S.A. Ackroyd-Stolarz, and P.B. Charlebois, "Influence of seat position on the static and dynamic forward and rear stability of occupied wheelchairs," *Arch. Phys. Med. Rehabil.*, vol. 74, pp. 977-982, 1993.

[13] R.L. Kirby, M.T. Sampson, F.A.V. Thoren, and D.A. MacLeod, "Wheelchair stability: effect of body position," *J. Rehab. Res. Dev.*, vol. 32, no. 4, pp. 367-372, 1995.

[14] R.L. Kirby, B.D. Ashley, S.A. Ackroyd-Stolarz, "Static rear and forward stability of occupied wheelchairs: effect of the magnitude and position of added loads," (abstract) *Arch. Phys. Med. Rehabil.*, vol. 73, p. 1014, 1992.

[15] R.L. Kirby, S.M. Atkinson, and E.A. MacKay, "Static and dynamic forward stability of occupied wheelchairs: influence of elevated footrests and forward stabilizers," *Arch. Phys. Med. Rehabil.*, vol. 70, pp. 681-686, 1989.

[16] *Working Model v3.0.3*. Knowledge Revolution, San Mateo, California, 1995.

[17] W.T. Dempster, *Space Requirements of the Seated Operator: Geometrical, Kinematic, and Mechanical Aspects of the Body With Special Reference to the Limbs.* WADC Tech Report 55-159. Wright-Patterson Air Force Base, OH: Wright Air Development Center, July 1955.

[18] F.P. Beer and E.R. Johnston Jr., *Vector Mechanics for Engineers: Dynamics (2nd S.I. Metric Edition).* McGraw-Hill, Singapore, 1990.